

TO THE EDITOR:

Genetic characterization and drug sensitivity study of newly derived HGBL double/triple-hit lymphoma cell lines

Jibin Zhang,^{1,*} Tingting Wang,^{2,*} Kunal Shetty,^{1,*} Serhan Alkan,³ Senlin Xu,⁴ Qiang Gong,¹ Xuxiang Liu,¹ Yuping Li,¹ Zunsong Hu,⁵ Wendong Huang,⁴ Hans-Guido Wendel,⁶ Alex F. Herrera,⁷ Raju K. Pillai,¹ Joo Y. Song,¹ and Wing C. Chan¹

¹Department of Pathology, City of Hope, Duarte, CA; ²Department of Hematology, Beijing Friendship Hospital, Capital Medical University, Beijing China; ³Department of Pathology and Laboratory Medicine, Cedars Sinai, Los Angeles, CA; ⁴Arthur Riggs Diabetes & Metabolism Research Institute, and ⁵Department of Computational and Quantitative Medicine, City of Hope, Duarte, CA; ⁶Cancer Biology and Genetics Program, Memorial Sloan-Kettering Cancer Center, New York, NY; and ⁷Department of Hematology and Hematopoietic Cell Transplantation, City of Hope, Duarte, CA

As a poor-risk group of aggressive B-cell lymphomas (BCLs), high-grade BCLs harboring *MYC* and *BCL2* and/or *BCL6* rearrangements high grade B-cell lymphoma-double/triple-hit (HGBL-D/TH) are currently a subject of intense clinical and research interest. New drugs, particularly targeted therapeutic agents, are increasingly being developed and entering the clinic in recent years.¹ A panel of well-characterized HGBL-D/TH cell lines will be valuable for preclinical drug screening and development. There are so far few HGBL-D/TH cell lines that have comprehensive genomic data.²⁻⁴ Here, we reported 2 new double/triple-hit lymphoma (D/THL) cell lines named “COH-DHL1” and “COH-THL1” with comprehensive characterization.

COH-DHL1 and COH-THL1 were derived from 2 male patients at City of Hope, and both were Epstein-Barr virus (EBV)-negative, as shown by the Epstein-Barr nuclear antigen polymerase chain reaction assay (Figure 1A). Their doubling times were 47.8 hours and 27 hours, respectively (Figure 1B). When we injected 10 million cells of each cell line subcutaneously into NSG mice, all 3 replicates developed tumors within 3 weeks (Figure 1C). Fingerprinting showed that the 2 cell lines were unique without any identical cell lines in the Cellosaurus database (supplemental Figure 1 in the data supplement). Flow cytometry showed consistent immunophenotype between the 2 cell lines, their 1- and 2-month cultures, and their mice tumors in terms of CD45, CD19/CD20, and immunoglobulin light chains (supplemental Figure 2 and Figure 1D). For COH-THL1, whose original tumor was available, fingerprinting and flow cytometry also showed consistency with its origin (supplemental Figures 1B and 2B). All animal procedures in the mice experiment were in accordance with the guidelines and approved by the Administrative Panel on Laboratory Animal Care at City of Hope Comprehensive Cancer Center.

The 2 cell lines were further characterized with 2 other reported D/THL cell lines (DOGKIT⁵ and CS-THL1⁶) for comparison. We tested the sensitivity of the 4 cell lines along with Jijoye and D/THL cell line (SU-DHL6) to 10 drugs targeting *BCL2*, *MYC*, *BTK*, *PI3K*, or *CDK* (Figure 1E). *BCL2* is an important antiapoptotic protein that synergizes with other oncogenes, such as *MYC*, to promote lymphoma development and could be a critical factor for HGBL-D/TH survival. Inhibiting *BCL2* by potent BH3 mimetics such as ABT-199 demonstrated a remarkable clinical response in selected patients.⁷ This is also demonstrated by the higher sensitivity of the 5 HGBL-D/TH cell lines to ABT199, compared with Jijoye, which is a Burkitt lymphoma (BL) lacking *BCL2* expression.

MYC, as a key oncogene,⁸ likely plays a crucial role in HGBL-D/TH, making it an excellent therapeutic target. Although it is yet impossible to directly inhibit *MYC* function, many strategies have been employed to indirectly inhibit *MYC* activity. In this study, we attempted to: (1) impair *MYC* transcription by inhibiting the BRD4 (bromodomain-containing 4) using JQ-1⁹; (2) interfere with *MYC* mRNA translation using the eukaryotic initiation factor (eIF) 4A inhibitor silvestrol¹⁰; (3) reduce *MYC* protein stability using

Submitted 29 November 2021; accepted 1 June 2022; prepublished online on *Blood Advances* First Edition 10 June 2022; final version published online 31 August 2022. DOI 10.1182/bloodadvances.2021006709.

*J.Z., T.W., and K.S. contributed equally to this study as joint first authors.

The sequencing data have been deposited in NCBI's Sequence Read Archive database with accession number PRJNA818709 (<https://www.ncbi.nlm.nih.gov/sra/PRJNA818709>).

The full-text version of this article contains a data supplement.

© 2022 by The American Society of Hematology. Licensed under Creative Commons Attribution-NonCommercial-NoDerivatives 4.0 International (CC BY-NC-ND 4.0), permitting only noncommercial, nonderivative use with attribution. All other rights reserved.

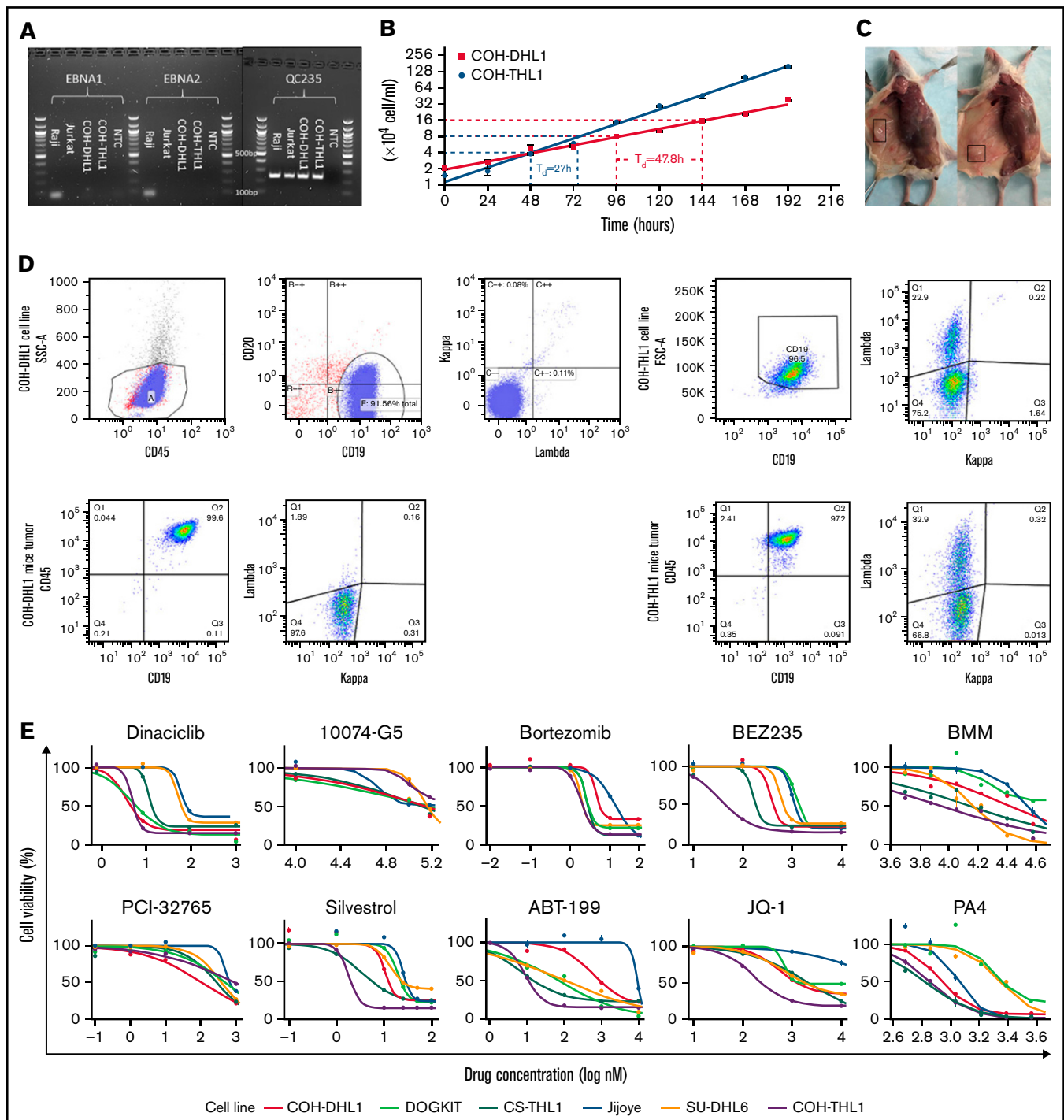


Figure 1. Characterization and validation of the D/THL cell lines. (A) EBNA (Epstein–Barr virus nuclear antigen 1) polymerase chain reaction assay of COH cell lines with negative control, an EBV-positive (Raji) and EBV-negative (Jurkat) cell line. QC235 is a positive control separately performed to confirm that DNA samples are amplifiable. (B) Growth plot for COH-DHL1 and COH-THL1 cell lines within 8 days with y-axis \log_2 transformed and doubling time (T_d) labeled. (C) Representative figure of mice with tumor highlighted in the box after subcutaneous injection of COH-DHL1 (left) and COH-THL1 (right). (D) Flow cytometry results of the 2 cell lines with their mice tumors. (E) Sigmoidal dose–response curves showing responses of 6 cell lines to 10 different drugs.

Berberamine¹¹ and its derivative PA4 through inhibition of the Ca^{2+} /calmodulin-dependent protein kinase γ 12; and (4) inhibit the transcriptional activity of MYC by disrupting its binding site using 10074-G5.¹³ Silvestrol was highly potent at the nM range. PA4

was quite promising (supplemental Table 1), whereas JQ1 and 10074-G5 were disappointing. Silvestrol is a flavagline that inhibits the activity of eIF4A subunit of the eIF4F complex. By inhibiting eIF4F, which is important for efficient translation of RNA containing

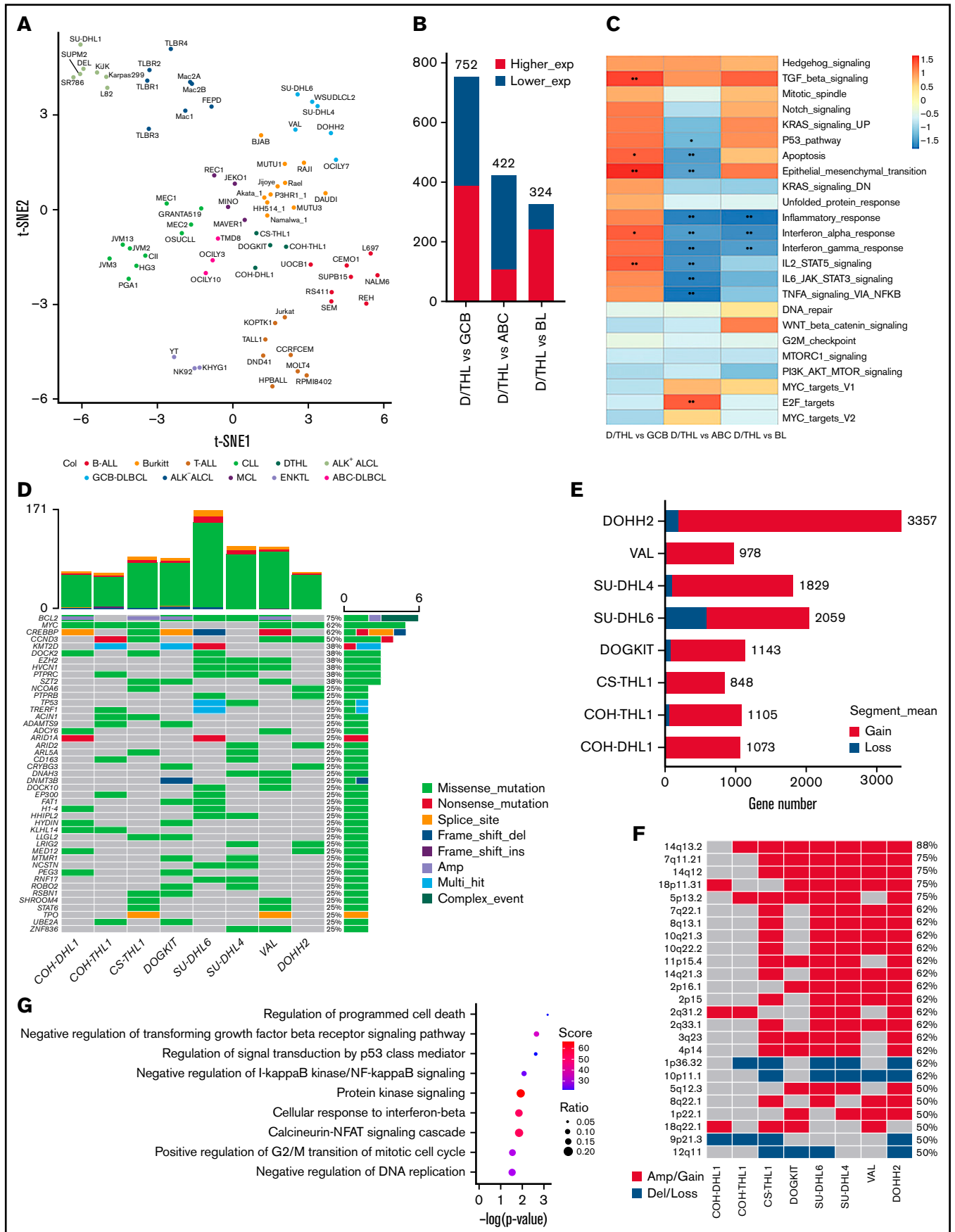


Figure 2.

G-quadruplex structures such as MYC and BCL2, silvestrol has shown powerful activities in human breast and prostate cancer xenograft models,¹⁴ as well as MYC-induced lymphomagenesis.¹⁵ All D/THL cell lines studied here were highly sensitive to silvestrol, indicating its potential as a powerful treatment option for D/THL.

Interestingly, the proteasome inhibitor bortezomib¹⁶ was a potent drug at the nM level, whereas the BTK inhibitor PCI-32765 and PI3K inhibitor BEZ235 required substantially higher concentrations. Dinaciclib, a novel drug that inhibits cyclin-dependent kinases CDK1, 2, 5, and 9,¹⁷ was also highly effective, especially for COH-DHL1, COH-THL1, and DOGKIT. This is consistent with the reported essential role of CDK9-mediated transcriptional elongation for tumor maintenance¹⁸ in a genetically defined MYC-driven model of hepatocellular carcinoma and downregulation of MCL-1¹⁹ and MYC²⁰ after CDK9 inhibition. In general, the COH cell lines were more responsive to most of the drugs. DHL6 tended to be more resistant, and Jijoye, which is a BL, had a different pattern of responses and tended to be the most resistant.

The 4 D/THL cell lines showed an average of 76 mutations with the most frequent alterations of MYC, BCL2, and CREBBP (supplemental Figure 3 and supplemental Table 2). Gene expression profiling of the 4 cell lines along with 74 other lymphoma/leukemia cell lines (supplemental Table 3) showed that their transcriptome profiles were close to BL, diffuse large B-cell lymphoma (DLBCL), and mantle cell lymphoma lines (Figure 2A and supplemental Figure 4A) with the highest similarity to BL cell lines (Figure 2B and supplemental Table 4). Gene set enrichment analysis showed enrichment of reported double-hit signature genes²¹ in D/THL compared with DLBCL and BL (supplemental Figure 4B-C). Differentially expressed genes in D/THL vs BL were significantly ($P < .05$) negatively enriched in the inflammatory response and interferon α and γ response, which was also true vs activated B-cell like-DLBCL. However, the opposite was observed when compared with germinal center B-cell like (GCB)-DLBCL, in which enrichment in multiple pathways such as the TP53 pathway, apoptosis, epithelial-mesenchymal transition, TGFB, and IL2/STAT5 signaling was also observed for D/THL (Figure 2C). The more prominent activation of the interferon pathways in BL could be related to the presence of EBV²² in many BL lines or more activation of endogenous retroviral elements in the BL cells.²³

We included 4 additional reported HGBL-D/TH cell lines (SU-DHL6, SU-DHL4, VAL, and DOHH2)² for genetic analysis. These cell lines showed more genetic abnormalities than the COH cell lines (Figure 2D-F), indicating that many acquired changes may have occurred because of in vitro culture, and it is important to use

lines with low passage numbers for study to avoid the noise from the artifactual changes. A few frequently mutant genes (eg, CREBBP, EZH2, KMT2D, and EP300) in these cell lines were shared with follicular lymphoma and GCB-DLBCL, consistent with the tumor derivation from GCB cells and the hypothesis that after acquiring the BCL2 translocation, the cells may evolve toward a GCB-like lymphoma with the acquisition of these mutations²⁴ (Figure 2D). The acquisition of the MYC translocation then drives the evolution to HGBL-D/TH in concert with the BCL2 translocation. There are other detected mutations (eg, TP53, PIM1, BAX, and CCND3) that may arise before or after the MYC translocation and further enhance MYC-driven cell cycle progression and cell survival. Importantly, our recent study found that HGBL-D/TH cases with TP53 abnormalities have a much worse prognosis.²⁵ GISTIC (Genomic Identification of Significant Targets in Cancer) identified 25 minimal common regions (MCRs) with genomic copy number abnormalities in ≥ 4 samples (Figure 2F). Among these, loss of 9p21 harboring CDKN2A and CDKN2B and gain of 2q31 were found in both COH cell lines; gains of 18p11 and 18q22 were in COH-DHL1; gains of 5p13 and 14q13 with NFKBIA; and loss of 1p36 containing TNFRSF14 were in COH-THL1. Genes in these MCRs are enriched in biological processes, including apoptosis, cell cycle and cytokine, TP53, TGF β (transforming growth factor β) receptor, NF- κ B (nuclear factor kappa B), protein kinase A, and IFN- β (interferon β) signaling (Figure 2G). We can envision that with a sufficient number of cell lines, we can further dissect different genetic/biological subgroups in vitro.

In conclusion, we established 2 new D/THL cell lines, COH-DHL1 and COH-THL1, and described their genetic characteristics as well as those of 2 additional cell lines, CS-THL1 and DOGKIT. We studied the sensitivity to 10 targeted agents using a D/THL cell line panel and demonstrated the potential of cell line models in preclinical studies of novel therapeutic agents that may benefit patients with HGBL-D/TH.

Acknowledgments: The authors thank Zhaohui Gu at the Department of Computational and Quantitative Medicine, City of Hope, for his valuable suggestions on data analysis and the staff of the Flow Cytometry Core, the Integrative Genomics Core, and Animal Tumor Model Core for their experimental assistance.

This work was supported by the National Cancer Institute of Health under grant number P30CA033572. It was also partly supported by Start-up funds from the City of Hope National Medical Center, the Dr. Norman and Melinda Payson Professorship in Hematologic Cancers, the Toni Stephenson Lymphoma Center, and the Nesvig fund.

Figure 2 (continued) Gene characterization of 4 D/THL cell lines compared with the other lymphoma/leukemia cell lines. (A) *t*-SNE clustering of the COH cell lines along with other 74 cell lines of 11 types. (B) The number of differentially expressed genes ($|\log_2$ fold change > 1 , false discovery rate < 0.1) for contrasts between D/THL and activated B-cell like (ABC)-DLBCL, GCB-DLBCL, or BL. (C) Heatmap showing gene set enrichment analysis results with hallmark gene sets for differentially expressed genes between D/THL, ABC-DLBCL, GCB-DLBCL, and BL. Gradient colors represent the net enrichment score. * $P < .05$; ** $P < .01$. (D) Waterfall plot showing the recurrent mutations in the 4 D/THL cell lines and the other 4 double-hit GCB-DLBCL cell lines. Different colors represent different types of mutations or CNA. The top bar plot shows the total number of mutations in each sample. The right bar plot shows the number of different alterations for each gene labeled by the percentage of samples that have genetic alteration in the gene. "Multi_Hit" means genes with cooccurring mutations of different types. "Complex_Event" means genes with both mutations and CNAs. (E) Bar plot showing expressed gene number covered by regions with copy number gain or loss of D/THL cell lines studied here along with another 4 double-hit cell lines. (F) Heatmap showing the distribution of the MCRs identified by GISTIC among the 8 cell lines. (G) The significant gene ontology (GO) terms ($P < .05$) enriched by the expressed genes in the MCRs ranked according to $-\log_{10}$ (P values) from top to bottom. The color and size of the dots indicate the enrichment score and ratio between gene number in MCRs and gene number in each GO term, respectively.

Contribution: J.Z., T.W., K.S., Y.L., A.F.H., J.Y.S., and W.C.C. drafted the manuscript and prepared the figures; W.C.C. designed and supervised the study; R.K.P., W.H., J.Y.S., H.-G.W., and S.A. provided cell lines and drugs; T.W., K.S., S.X., and Y.L. conducted cell culture and drug response experiments; J.Y.S. and K.S. conducted flow cytometry and PCR experiments; K.S. and X.L. conducted mouse study; J.Z., Q.G., and Z.H. are involved in the bioinformatic analysis; and the manuscript has been read and approved for submission by all authors.

Conflict-of-interest disclosure: The authors declare no competing financial interests.

ORCID profiles: J.Z., 0000-0003-3099-6665; K.S., 0000-0003-1065-2734; S.A., 0000-0002-4483-2576; S.X., 0000-0001-6625-5370; Q.G., 0000-0001-8502-6813; X.L., 0000-0002-1677-0814; Y.L., 0000-0002-6514-6719; Z.H., 0000-0003-3167-7148; W.H., 0000-0003-3735-9466; H.-G.W., 0000-0001-7166-4670; A.F.H., 0000-0002-9665-7415; J.Y.S., 0000-0003-3497-2513; W.C.C., 0000-0002-6243-6008.

Correspondence: Wing C. Chan, Department of Pathology, City of Hope National Medical Center, Duarte, CA 91010; e-mail: jochan@coh.org; Joo Y. Song, Department of Pathology, City of Hope National Medical Center, Duarte, CA 91010; e-mail: josong@coh.org; and Raju K. Pillai, Department of Pathology, City of Hope National Medical Center, Duarte, CA 91010; e-mail: rpillai@coh.org.

References

1. Smith AD, Roda D, Yap TA. Strategies for modern biomarker and drug development in oncology. *J Hematol Oncol*. 2014;7(1):70.
2. Drexler HG, Eberth S, Nagel S, MacLeod RA. Malignant hematopoietic cell lines: in vitro models for double-hit B-cell lymphomas. *Leuk Lymphoma*. 2016;57(5):1015-1020.
3. Li W, Gupta SK, Han W, et al. Targeting MYC activity in double-hit lymphoma with MYC and BCL2 and/or BCL6 rearrangements with epigenetic bromodomain inhibitors. *J Hematol Oncol*. 2019;12(1):73.
4. Drexler HG, Quentmeier H. The LL-100 cell lines panel: tool for molecular leukemia-lymphoma research. *Int J Mol Sci*. 2020;21(16):5800.
5. Kiefer T, Schüler F, Knopp A, et al. A human Burkitt's lymphoma cell line carrying t(8;22) and t(14;18) translocations. *Ann Hematol*. 2007;86(11):821-830.
6. Cinar M, Rosenfelt F, Rokhsar S, et al. Concurrent inhibition of MYC and BCL2 is a potentially effective treatment strategy for double hit and triple hit B-cell lymphomas. *Leuk Res*. 2015;39(7):730-738.
7. Roberts AW, Huang D. Targeting BCL2 with BH3 mimetics: basic science and clinical application of venetoclax in chronic lymphocytic leukemia and related B cell malignancies. *Clin Pharmacol Ther*. 2017;101(1):89-98.
8. Koh CM, Sabò A, Guccione E. Targeting MYC in cancer therapy: RNA processing offers new opportunities. *BioEssays*. 2016;38(3):266-275.
9. Roderick JE, Tesell J, Shultz LD, et al. c-Myc inhibition prevents leukemia initiation in mice and impairs the growth of relapsed and induction failure pediatric T-ALL cells. *Blood*. 2014;123(7):1040-1050.
10. Wiegner A, Uthe FW, Jamieson T, et al. Targeting translation initiation bypasses signaling crosstalk mechanisms that maintain high MYC levels in colorectal cancer. *Cancer Discov*. 2015;5(7):768-781.
11. Gu Y, Chen T, Meng Z, et al. CaMKII γ , a critical regulator of CML stem/progenitor cells, is a target of the natural product berbamine. *Blood*. 2012;120(24):4829-4839.
12. Gu Y, Zhang J, Ma X, et al. Stabilization of the c-Myc protein by CAMKII γ promotes T cell lymphoma. *Cancer Cell*. 2017;32(1):115-128.e7.
13. Yin X, Giap C, Lazo JS, Prochownik EV. Low molecular weight inhibitors of Myc-Max interaction and function. *Oncogene*. 2003;22(40):6151-6159.
14. Cencic R, Carrier M, Galicia-Vázquez G, et al. Antitumor activity and mechanism of action of the cyclopenta[b]benzofuran, silvestrol. *PLoS One*. 2009;4(4):e5223.
15. Alinari L, Prince CJ, Edwards RB, et al. Dual targeting of the cyclin/Rb/E2F and mitochondrial pathways in mantle cell lymphoma with the translation inhibitor silvestrol. *Clin Cancer Res*. 2012;18(17):4600-4611.
16. Chen D, Frezza M, Schmitt S, Kanwar J, Dou QP. Bortezomib as the first proteasome inhibitor anticancer drug: current status and future perspectives. *Curr Cancer Drug Targets*. 2011;11(3):239-253.
17. Kumar SK, LaPlant B, Chng WJ, et al; Mayo Phase 2 Consortium. Dinaciclib, a novel CDK inhibitor, demonstrates encouraging single-agent activity in patients with relapsed multiple myeloma. *Blood*. 2015;125(3):443-448.
18. Huang CH, Lujambio A, Zuber J, et al. CDK9-mediated transcription elongation is required for MYC addiction in hepatocellular carcinoma. *Genes Dev*. 2014;28(16):1800-1814.
19. Gregory GP, Hogg SJ, Kats LM, et al. CDK9 inhibition by dinaciclib potently suppresses Mcl-1 to induce durable apoptotic responses in aggressive MYC-driven B-cell lymphoma in vivo. *Leukemia*. 2015;29(6):1437-1441.
20. Moharram SA, Shah K, Khanum F, Marhäll A, Gazi M, Kazi JU. Efficacy of the CDK inhibitor dinaciclib in vitro and in vivo in T-cell acute lymphoblastic leukemia. *Cancer Lett*. 2017;405:73-78.
21. Ennishi D, Jiang A, Boyle M, et al. Double-hit gene expression signature defines a distinct subgroup of germinal center B-cell-like diffuse large B-cell lymphoma. *J Clin Oncol*. 2019;37(3):190-201.
22. Liu X, Sadaoka T, Krogmann T, Cohen JL. Epstein-Barr virus (EBV) tegument protein BGLF2 suppresses type I interferon signaling to promote EBV reaction. *J Virol*. 2020;94(11):e00258-e20.
23. Sutkowski N, Chen G, Calderon G, Huber BT. Epstein-Barr virus latent membrane protein LMP-2A is sufficient for transactivation of the human endogenous retrovirus HERV-K18 superantigen. *J Virol*. 2004;78(14):7852-7860.
24. Cucco F, Barrans S, Sha C, et al. Distinct genetic changes reveal evolutionary history and heterogeneous molecular grade of DLBCL with MYC/BCL2 double-hit. *Leukemia*. 2020;34(5):1329-1341.
25. Song JY, Perry AM, Herrera AF, et al. Double-hit signature with TP53 abnormalities predicts poor survival in patients with germinal center type diffuse large B-cell lymphoma treated with R-CHOP. *Clin Cancer Res*. 2021;27(6):1671-1680.